Applied Soft Computing 10 (2010) 135–148

Contents lists available at ScienceDirect

Applied Soft Computing

journal homepage: www.elsevier.com/locate/asoc

Neural networks modeling of shear strength of SFRC corbels without stirrups

Shailendra Kumar [a,b], S.V. Barai [b,*]

[a] Department of Civil Engineering, National Institute of Technology, Jamshedpur 831014, India
[b] Department of Civil Engineering, Indian Institute of Technology, Kharagpur, Kharagpur, West Bengal 721302, India

ARTICLE INFO

Article history:
Received 7 April 2008
Received in revised form 14 April 2009
Accepted 28 June 2009
Available online 3 July 2009

Keywords:
Artificial neural network
Fiber reinforced concrete
Reinforced concrete corbels
Shear strength
Stirrups

ABSTRACT

Based on developed semi-empirical characteristic equations an artificial neural network (ANN) model is presented to measure the ultimate shear strength of steel fibrous reinforced concrete (SFRC) corbels without shear reinforcement and tested under vertical loading. Backpropagation networks with Lavenberg–Marquardt algorithm is chosen for the proposed network, which is implemented using the programming package MATLAB. The model gives satisfactory predictions of the ultimate shear strength when compared with available test results and some existing models. Using the proposed networks results, a parametric study is also carried out to determine the influence of each parameter affecting the failure shear strength of SFRC corbels with wide range of variables. This shows the versatility of ANNs in constructing relationship among multiple variables of complex physical relationship.

1. Introduction

Artificial neural network (ANN) is a system of parallel processor that mimics the working procedure of the human brain in which billions of neurons are connected in a complex manner and each neuron receives signal through synapses that control the effects of other neurons. Thus, networks of the artificial neurons inspired by a physioneural model are the system composed of many simplified processing elements which operate in parallel whose function is determined by network architect, connecting strength and processing performed at computing nodes or neurons. Through learning ability of the networks directly from experimental or numerically obtained data, the potential knowledge is stored in connecting weights as distributed memory. Hence, the ANN may be inserted into analytical codes to predict the outputs as a function of input parameters after training according to the experimental or numerical data without the benefit of best-fit analysis. The neural networks can be efficiently used for more extended nonlinear as well as multidimensional problems which do not need a specific equation form. Instead, the networks require sufficient input–output data or experimental results or experience which can be continuously retrained and updated as and when the new data or results or experiences are made available in the future.

In the recent past, ANN has been successfully applied in various disciplines of engineering analysis including in the field of Civil Engineering such as structural engineering problems. The major concerns of a structural engineer including structural analysis problems, predicting different properties of concrete and estimating the load carrying capacity of concrete structures have been solved by mostly using the backpropagation neural networks (BPNN). Waszczyszyn and Ziemiański [49] used BPNN to solve many problems of structural mechanics. Within an allowable error, a neural-networks-based model for approximate structural analysis was developed and verified to predict the behavior of a stub-girder system [34].

Different ANN models [30,28,50,23,33,31] were proposed for determining strength of concrete using design mix parameters. In addition, a model was constructed by using ANN and experimental results to determine the properties of waste autoclaved aerated concrete aggregate concrete [48]. ANN was also used to predict the elastic modulus of normal and high strength concrete [13]. Neural networks study was carried out to predict compressive strength of granulated blast furnace slag concrete [6]. Sarıdemir [44] developed ANN models for predicting compressive strength of concrete containing metakaolin and silica fume at different ages. Raghu Prasad et al. [41] presented an ANN approach to determine a 28-day compressive strength of a normal and high strength self-compacting concrete and high performance concrete with high volume fly ash. A multi-layer feed-forward neural network was established to determine the ultrasonic pulse velocity–strength relationship of concrete [47]. The results showed that ANN can be a useful tool for predicting the concrete strength and its properties within an acceptable error. ANN modeling was also applied in several concrete structures for the prediction of capacity of pin-ended reinforced concrete (RC) column [8], deflection of externally

* Corresponding author. Tel.: +91 3222 283408; fax: +91 3222 282254.
E-mail addresses: shailendrakmr@yahoo.co.in (S. Kumar), skbarai@civil.iitkgp.ernet.in (S.V. Barai).

1568-4946/$ – see front matter © 2009 Elsevier B.V. All rights reserved.
doi:10.1016/j.asoc.2009.06.012

Nomenclature

A_S	total area of tensile steel
b	width of cross-section of corbel
C	total compressive force
d	effective depth of corbel
d_f	fiber diameter
E_c	modulus of elasticity of concrete matrix
E_s	modulus of elasticity of steel = 210 KN/mm^2
F_1, F_2, F_3, F_4 and $F(\alpha)$	functional notations as defined in the text
F_t	total tensile force
F_{ft}	tensile force in fibrous concrete composite
F_{st}	tensile force in conventional tension steel
f_a	average longitudinal concrete stress over a small stretch
v_a	average shear stress in concrete over a small stretch
f'_c	compressive strength of standard cylinder of concrete matrix
f''_c	maximum compressive stress in concrete matrix in flexural = 0.85 f'_c
f_{sc}	total steel stress at shear cracking
j	lever arm factor
k	neutral axis depth factor
k_b	bond length coefficient = 58
k_1	ratio of average compressive stress to f''_c
k_2	ratio of depth of compression force to effective depth
l_f	fiber length
m	modular ratio
V_u	ultimate shear force of corbel without shear reinforcement
p_t	A_s/bd = tensile reinforcement ratio
v_f	percentage volume fraction of fibers

Greek symbols

α	plasticity coefficient = $\varepsilon_{cc}/\varepsilon_{ce}$
ε_{cc}	top concrete strain at shear cracking
ε_{ce}	strain at which concrete becomes plastic
ε_s	steel strain corresponding to steel stress f_{sc}
η_b	bond efficiency factor
η_l	length correction factor
η_o	fiber orientation factor
σ_{cu}	ultimate strength in tension of fibrous concrete composite
θ	angle between inclined compressive force and resultant tensile force
τ	interfacial bond stress between fiber and concrete
$\tau_u = V_u/bd$	ultimate shear strength of corbel without shear reinforcement

reinforced RC beams [20] and modeling the confined strength and strain of circular columns [37]. Hadi [24] used backpropagation networks to train the networks for the optimum design of simply supported RC beams with and without steel fibers under different loadings and configurations.

A structural engineer faces difficulty to determine the accurate load carrying capacity of reinforced concrete structures failing under shear. Although, considerable advancement has taken place in the last few decades in this area, research work is still in progress for understanding the complex behavior of RC beams subjected under predominating shear force because of several important parameters affecting the intricate shear transfer mechanism. Most of national codes for shear design are still based on the empirical formulae and they vary significantly from code to code hence there is a lack of consistency in factor of safety against shear capacity of RC beams. Perhaps these reasons prompted several researchers [22,43,42,5,9,10,35,38,7,11,4,29] around the world to implement ANN based approach for predicting the ultimate shear capacity of RC beams with and without stirrups. Most of the neural network models are able to simulate the structural behavior observed in the experimental results of RC beams subjected to predominant shear failure. The parameters that affect the shear resistance mechanisms without shear stirrups are normally concrete strength, longitudinal reinforcement ratio, depth of the beam, width of the beam, shear-span to depth ratio, yield strength of longitudinal reinforcement, etc. In addition, transverse reinforcement ratio and yield strength of the stirrups also influence in the total contribution of shear resistance of the RC beams with shear stirrups. Addition of steel fibers improves the concrete in compression, tension and shear. The crack-arresting action of steel fibers in concrete results in improved performance of steel fiber reinforced concrete. These fibers are randomly distributed throughout the volume of concrete at much closer spacing. Hence, two more important parameters volume fraction and aspect ratio of steel fibers also affect the shear resistance of SFRC concrete beams in addition to the previously mentioned parameters. Among all, shear-span depth ratio is one of the important parameters which influence the shear capacity of RC beams significantly and, normally the shear resistance increases as the shear-span depth ratio decreases. The structural members such as cantilever beams with a shear-span depth ratio normally less than unity and projecting out from faces of RC columns are known as corbels or brackets. They are extensively used in precast concrete construction to support primary beams and girders and hence facilitating the transfer of force from the beams (and girders) to the column members.

In the past limited methodologies such as ACI building code method [3], truss analogy method [25] and modified shear-friction equation [15] have been used by Abdul-Wahab [1] for the analysis of tested corbels containing primary and secondary (stirrups) reinforcement with different types of steel fibers of varying volume fractions. Fattuhi and Hughes [18] presented an empirical equation based on a statistical analysis for prediction of corbel strength made of primary steel and with and without fibers. The volume fraction of steel fibers was kept constant as 0.70%. The derived equation is applicable to corbels with similar reinforcements and concrete used in the study. In the investigation by Fattuhi [16], it was also concluded that loading the column segment of the specimen or the left side corbel did not appear to have any significant effect on the load carrying capacity of the failed (right side) corbel. Fattuhi [17] put forward a single generalized empirical equation based on regression analysis for strength estimation of corbels containing primary steel and with and without fibers. The shear strength of reinforced fibrous concrete corbels without shear stirrups has also been analyzed on a rational basis involving wide range of parameters [32].

It is evident from the past literature that the several complex modes of shear failures involving large number of parameters have been identified and at the same time, no closed form equation is available for predicting the shear strength of SFRC corbels without shear stirrups subjected to vertical loads. In addition, one has to rely on the empirical or semi-empirical equations based on the regression analysis which can be applicable to the similar

conditions and may be doubtful for the general applications. Furthermore, it is difficult to identify the exact shear transfer mechanism of SFRC corbels because of the redistributions of complex stresses that take place during the crack initiation and its growth phenomena. Such circumstances are favorable for the potential applications of the ANN based approach to facilitate a systematic and rapid assessment of the behavior of SFRC corbels without web reinforcement or stirrups, subjected to vertical loading. The ANN has capability to learn the relation between input and output automatically, provided sufficient data is available for its training. Therefore, the main objective of the present paper is to develop the ANN models for predicting the shear capacity of SFRC corbels without shear stirrups and subjected to the vertical loads. In addition, a parametric study is also carried out using ANN model to verify whether the predicted results are in consistent with the expected experimental observations. Based on the detailed literature review, following objectives have been identified for the present paper:

1. Study and identification of problem domain
2. Data collection for the problem domain
3. Implementation of neural network and
4. Study of the performance of the neural network model.

Semi-empirical characteristic equations [32] have been used to develop the database for the networks training for which 730 numbers of data sets of different cross-sections of corbels are randomly created. Three-layer feed-forward neural networks are developed using backpropagation with Lavenberg–Marquardt learning algorithm [14] which is implemented using the programming package MATLAB. The networks are tested on the new data sets obtained from the experimental results [16–19,27]. Results obtained from ANN determines (i) the ultimate shear strength of steel fibrous reinforced concrete corbels under vertical loads; (ii) the comparison with the experimental results and (iii) the impact of various parameters on shear strength.

2. Study and identification of problem domain

2.1. Analysis of shear strength of SFRC corbels

The cross-sectional details, general arrangement of reinforcements and potential cracking pattern at shear failure of a typical reinforced concrete corbel is shown in Fig. 1. Because corbel dimensions are small, special attention must be paid to providing proper anchorage for all bars. It is designed for the vertical reaction V_u and horizontal force N_u unless special precautions are taken to avoid horizontal forces due to restrained shrinkage, creep or temperature change. One of the complex mechanisms during shear failure of a reinforced concrete corbels is that it develops a diagonal crack during shear failure. Second possible mode of failure is the direct shear along a plane more or less flush with the vertical face of the main part of the column. Different types of failure mechanisms, crack patterns and the design of reinforced concrete corbels have been mentioned elsewhere [39]. The failure process of reinforced concrete corbels with or without steel fibers is fairly complex as evident from the analysis of test results carried out by Fattuhi and Hughes [19]. The study showed that corbels with plain concrete failed in flexure manner whereas corbels with main bars failed after exhibiting multiple cracks on both sides of the column showing mainly four types of failure modes: flexure, flexure-shear, inclined shear and diagonal splitting. The corbels reinforced with main bars only failed by diagonal splitting whereas corbels reinforced with stirrups along with the main bars failed in inclined shear. Depending upon the percentage reinforcement, mixed type of failure modes were observed when corbels were reinforced with steel fibers in addition to the main bars.

General dimensions and loading conditions of a SFRC corbel without stirrups taken up in the study is shown in Fig. 2. In the figure, b is width, d is effective depth and h is the total depth of the rectangular cross-section of a corbel, a is shear-span and A_s is the area of primary or main reinforcements. The influencing parameters of the shear resistance are concrete strength f'_c, b, d, shear-span depth ratio a/d, main reinforcement ratio $p_t = A_s/bd$ and fiber properties such as volume fraction v_f and fiber aspect ratio l_f/d_f. In the present study, the horizontal force N_u is neglected and assumed that the corbel is primarily subjected to vertical shear force V_u. Normally, shear capacity V_u of SFRC corbels without shear stirrups increases as concrete strength f'_c increases. The V_u also increases with the increase in cross-sectional areas ($b \times d$), decrease in the a/d ratio and increase in the main reinforcement ratio p_t of the corbels. The shear capacity further increases with increase in fiber content in the fiber reinforced concrete. These geometrical and material properties are mainly considered as the known parameters while analysis of the test results and predicting the shear strength of the corbels. The preceding information may be helpful while formulating the problem as considered in the present investigation using ANN approach. The explanation of cracking mechanism and the simplification assumed for the present analysis are mentioned in Appendix A. Based on the complex cracking phenomena and simplified assumptions at the failure of the SFRC corbel, the following semi-empirical formulae [32] are arrived at for predicting the ultimate shear capacity

$$\frac{k_1 k}{[1+\{(1-k_2 k)d/a\}^2]^{1/2}} = p_t m\alpha\left(\frac{1-k}{k}\right) + \frac{\eta_o \eta_b \eta_l (l_f/d_f) v_f 2\tau(1-k)}{0.85 f'_c} \quad (1)$$

In which, k is the neutral axis depth factor, α is the plasticity coefficient; k_2, η_o, η_b, η_b are some constants as given in Appendix A; $m = E_s/E_c$ = modular ratio, E_s and E_c are the moduli of elasticity of

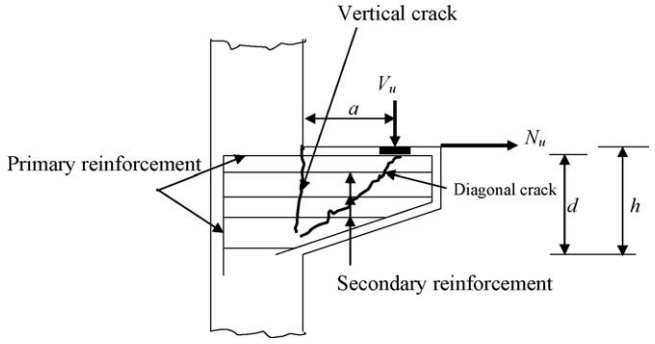

Fig. 1. Cracking pattern at shear failure of a typical reinforced concrete corbel.

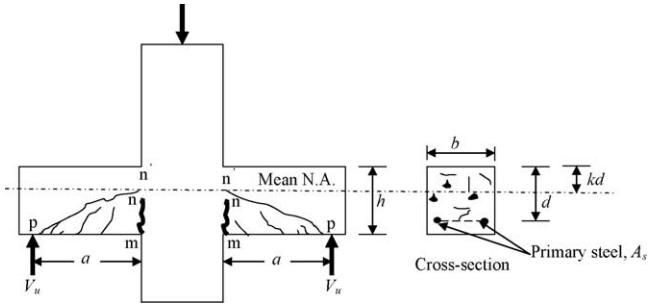

Fig. 2. Initiation of cracks at shear failure of SFRC corbel.

main steel reinforcement and concrete respectively. Also,

$$k_1 = \frac{\alpha}{2} \quad \text{and} \quad k_2 = \frac{1}{3} \quad \text{when } \alpha \le 1 \tag{2}$$

and

$$k_1 = \frac{2\alpha - 1}{2\alpha} \quad \text{and} \quad k_2 = \frac{1}{2k_1}\left[1 - \frac{1}{\alpha} + \frac{1}{3}\left(\frac{1}{\alpha}\right)^2\right] \quad \text{when } \alpha \ge 1 \tag{3}$$

The constant k can be expressed as

$$k_1 = \frac{V_u a}{kjbd^2 f_c'' \cos\theta} \tag{4}$$

Finally, the α is expressed as

$$\alpha = \frac{2V_u a}{kjbd^2 f_c'' \cos\theta} \quad \text{when } \alpha \le 1 \tag{5}$$

and

$$\alpha = \frac{1}{2\left(1 - V_u a / kjbd^2 f_c'' \cos\theta\right)} \quad \text{when } \alpha \ge 1 \tag{6}$$

where θ is the angle between the total compressive force C and the total tensile force F_t in the strut-tie model as shown in Appendix A (Fig. A1). For a particular corbel test, values of k and corresponding α at observed V_u may be calculated with the help of Eqs. (1)–(3), (5) and (6), using trial and error method in which a suitable value of α is initially assumed. The non-dimensional shear strength in functional form can be expressed as

$$F(\alpha) = \frac{V_u a}{kbd^2 f_c'' \cos\theta} = 0.4360\alpha^{0.6963} \quad \text{when } \alpha \le 1.36 \tag{7}$$

and

$$F(\alpha) = \frac{V_u a}{kbd^2 f_c'' \cos\theta} = 0.5092\alpha^{0.1913} \quad \text{when } \alpha \ge 1.36 \tag{8}$$

Finally, the non-dimensional coefficients k_1, j and α are related as

$$j = \frac{0.4360\alpha^{0.6963}}{k_1} \quad \text{when } \alpha \le 1.36 \tag{9}$$

and

$$j = \frac{0.5092\alpha^{0.1913}}{k_1} \quad \text{when } \alpha \ge 1.36 \tag{10}$$

Eqs. (9) and (10) may be designated as shear strength characteristic equations at shear cracking which are in excellent agreement [32] with the experimental results available in the literature [16–19,27]. For completeness of the paper and ready reference the derivation of the shear strength characteristic equations is presented in Appendix A. Eqs. (1)–(10) can be used to determine the ultimate shear capacity of a SFRC corbel with known material and geometrical properties.

2.2. Computation of shear strength

Based on Eq. (1), the dimensionless shear strength parameter $F(\alpha)$ and α are plotted in Fig. 3. This figure is known as corbel characteristic curve. To predict the ultimate shear capacity of a particular corbel with known properties, two unknown quantities k and α are to be determined with the help of Eqs. (1), (9) and (10). Simultaneous solutions of these equations are illustrated graphically in Fig. 4 and represented by the intersection of two curves, namely, the shear strength characteristic curve based on Eqs. (9) and (10), and the corbel characteristic curve (Fig. 3). A set of rules may be framed for rapid computation of shear failure load at converging values of α and j using shear strength characteristic curve (Fig. 4) or Eq. (9) or (10) and Eqs. (2)–(4) and either Eq. (5) or (6). Adopting the final converged quantities of α, j, k and $\cos\theta$ at ultimate shear strength, primary reinforcement ratio p_t is computed using Eq. (1). A flowchart showing systematic calculation for the above set rule is shown in Fig. 5.

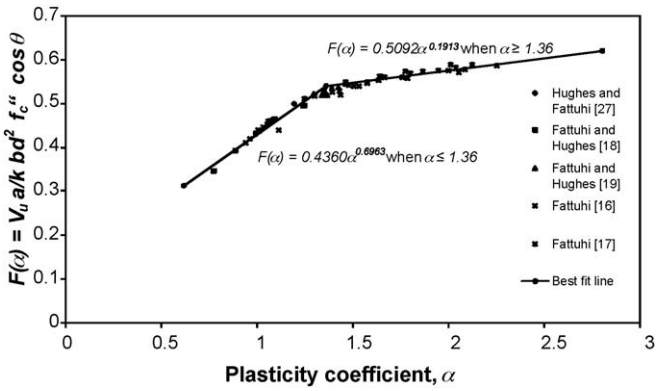

Fig. 3. Relationship between plasticity coefficient, α and $V_u a/kbd^2 f_c' \cos\theta$.

3. Data collection and neural network modeling

3.1. Network architecture

Artificial neural network may be defined as a structure composed of a number of interconnected units. Each unit has an input/output characteristic and implements a local computation or function. The output of any unit is determined by its input/output characteristic, its interconnection to other units and external inputs. The overall function or functionality of ANN achieved is determined by the topology, the individual neuron characteristics, and the learning or training strategy and training data. The processing units may be grouped into layers of input, hidden and output neurons. The most difficult task in the neural network design is to decide the number of hidden layers and number of nodes in the hidden layers. Since in the literature no specific guidelines are available, mostly trial and error method is adopted for the overall design of the networks. Mukherjee and Deshpande [36] proved that for the type of functional problem considered in this investigation, the use of one hidden layer or two hidden layers does not make any significant difference in terms of level of accuracy but it does differ in terms of time required for learning. In

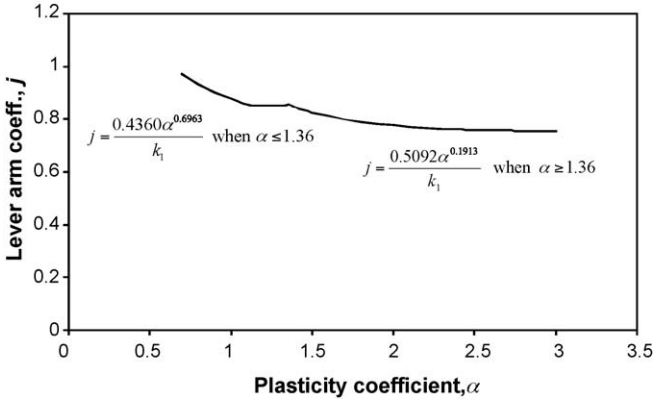

Fig. 4. Shear strength characteristic curve.

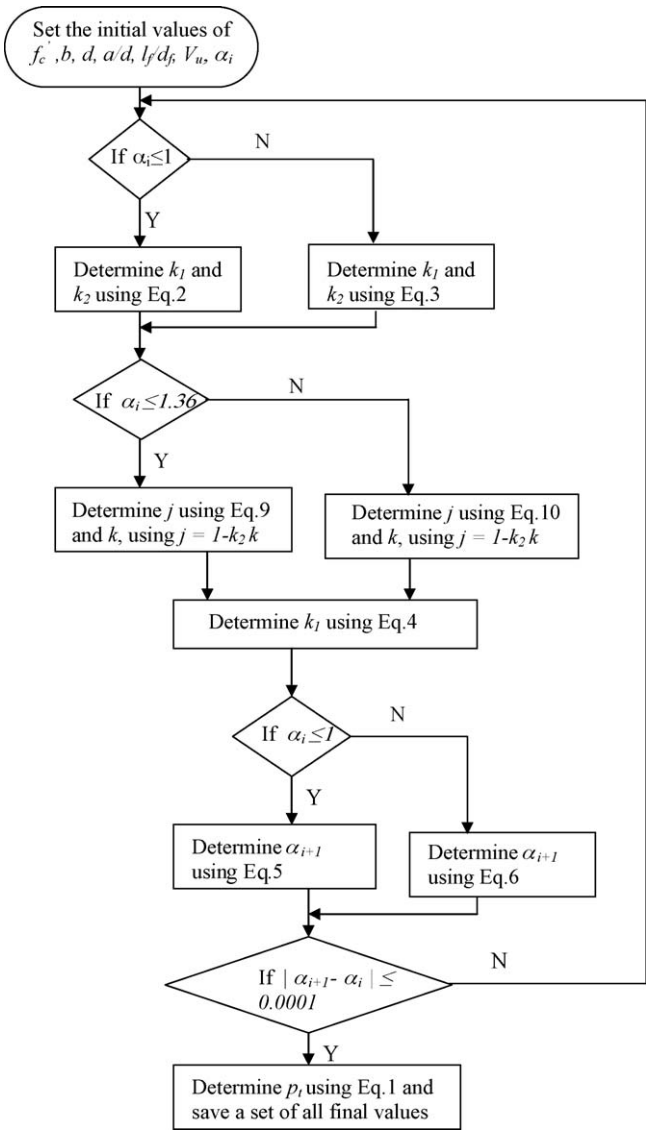

Fig. 5. Flowchart for computing database.

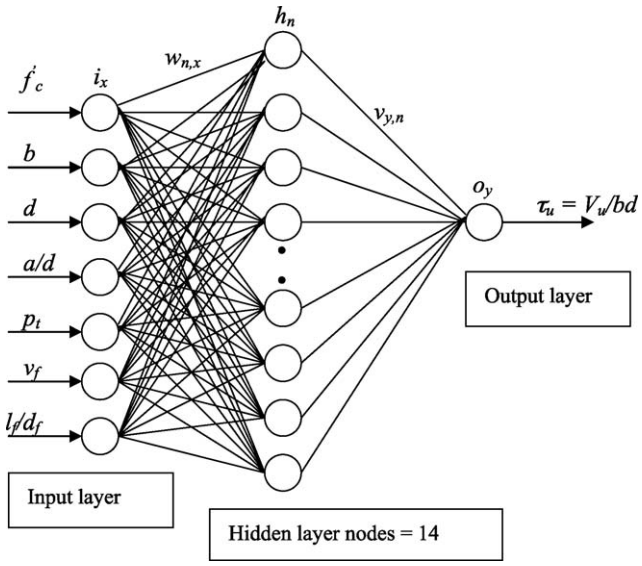

Fig. 6. Model of back-propagation for ultimate shear strength of reinforced concrete corbels.

the present case, after a few trials good convergence could be achieved with single hidden layer consisting of fourteen neurons. Hence, this configuration of the neural networks was retained for the study and prospective analysis. The adopted topology or architecture of a three-layer feed-forward neural network is presented schematically as shown in Fig. 6. The neural network in the figure consists of seven input neurons, one hidden layer with fourteen neurons and one output neuron. The strength of the connections among the processing units is provided by a set of weights and biases that affect the magnitude of the input which will be received by the neighboring units.

The following equations describe the mode of operation of a three-layer feed-forward network:

$$h_n = \phi(V_n) = \phi\left(\sum_{x=0}^{M} w_{n,x} i_x\right) = \phi\left(\sum_{x=1}^{M} w_{n,x} i_x + b_n\right) \quad (11)$$

$$o_y = \phi(V_y) = \phi\left(\sum_{n=0}^{N} v_{y,n} h_n\right) = \phi\left(\sum_{n=1}^{N} v_{y,n} h_n + b_y\right) \quad (12)$$

where i_x is the scaled input value transmitted from the xth input neuron; h_n is the activity level generated at the nth hidden neuron; o_y is the activity level generated at the yth output neuron; $w_{n,x}$ and $v_{y,n}$ are the weights on the connections to the hidden and output layers of neurons, respectively; b_n and b_y are the weighted biases and $\phi(V)$ is the activation function. In this case, the sigmoid function $\phi(V) = 1/[1 + \exp(-aV)]$ is taken into account.

Most neural network applications are based on the back-propagation paradigm, which uses the gradient descent method to minimize the error function. Although the back propagation algorithm based on gradient-descent method is simple, it is very slow in convergence. Numerical optimization theory provides a rich and robust set of techniques, which can be applied to neural networks to improve learning rates. The gradient-descent method considers only the first order derivative of an error function. The algorithm that considers the second order derivatives of the error function can further improve the rate of convergence. Lavenberg–Marquardt algorithm [14] is one such method, which uses second order derivatives of the error function and can be used as a variant of backpropagation to improve the learning rate. The weight update rule of this algorithm is given by (in vector notation)

$$\Delta w = (H + \mu \times I)^{-1} \times J^T \quad (13)$$

where $H = J^T \times J$ is the Hessian matrix of error vector and is equal to $\Delta^2 E$, J is the Jacobian matrix of derivatives of each error to each weight, μ is a small scales which controls the learning process, E is an error vector, Δw is the change in weights, J^T is the transpose of the Jacobian matrix and I is the identity matrix. If the scalar μ is very large, the above expression approximates gradient descent method, while if it is very small the above expression becomes Gauss–Newton method. Hence, μ is decreased after each successful step and is increased only when a step increase the error. In practice, Lavenberg–Marquardt algorithm [14] with backpropagation (LMBP) is faster and finds better optima for a variety of problems than other usual methods and hence in the present study the same algorithm has been used. Details of the backpropagation procedure can be found in the literature [26].

3.2. Database for training of network

Based on previous analysis the shear strength computation is performed using a set of Eqs. (9) or (10) along with Eq. (5) or (6) and then the primary steel ratio is determined using Eq. (1) (Fig. 5).

Table 1
Database for training of ANN.

Corbel section, $b \times d$ (mm × mm)	Range	f'_c (MPa)	a/d	p_t (%)	Fiber properties		V_u (kN)	τ_u (MPa)	No. of data
					v_f (%)	l_f/d_f			
100 × 125	Maximum	33.5	1.16	1.613	3.35	104.0	95.0	7.60	60
	Minimum	20.0	0.4	0.267	0.50	50.0	50.0	4.00	
125 × 100	Maximum	52.0	1.15	2.478	3.22	111.0	150.0	12.00	50
	Minimum	25.0	0.4	0.185	0.52	48.0	40.0	3.20	
125 × 150	Maximum	37.5	1.24	1.858	3.35	104.0	195.0	10.40	140
	Minimum	24.0	0.4	0.170	0.50	50.0	60.0	3.20	
150 × 125	Maximum	52.0	1.16	2.145	3.22	111.0	219.0	11.68	60
	Minimum	25.0	0.4	0.13	0.52	48.0	50.0	2.67	
150 × 200	Maximum	48.0	1.15	2.229	3.35	104.0	359.0	11.97	220
	Minimum	30.0	0.4	0.106	0.50	50.0	85.0	2.83	
200 × 150	Maximum	52.0	1.16	1.379	3.22	111.0	323.0	10.77	70
	Minimum	25.0	0.4	0.10	0.52	48.0	70.0	2.33	
200 × 250	Maximum	62.0	1.16	2.667	3.22	113.0	780.0	15.6	80
	Minimum	35.0	0.4	0.21	0.52	50.0	200.0	4.00	
225 × 300	Maximum	62.0	1.15	2.982	3.22	113.0	1025.0	15.19	50
	Minimum	35.0	0.4	0.439	0.52	50.0	400.0	5.93	

Seven numbers of various cross-sections of corbels are arbitrarily chosen for this study and with different properties of each cross-section of the corbel; the values of the shear strength and primary reinforcement ratios are computed. As such for the training of networks 730 number of data set are prepared which are shown in Table 1. Initially the data set was computed at smaller step sizes for the corbel cross-sections 125 mm × 150 mm and 150 mm × 200 mm which gave rise to 140 and 220 numbers of input data sets respectively. If the same number of data sets were calculated for other corbel cross-sections the number of input data sets would be relatively large. Therefore, the input data sets for other cross-sections of corbels were reduced by increasing the step sizes in the calculation so that reasonable number of total data sets could be obtained. Since, this particular set of input data gave good results in the ANN modeling; the same data sets were retained in the study. The range of maximum and minimum values of each variable to be used in the study is presented in Table 2. With this data set (Table 1) at shear failure of SFRC corbels subjected to vertical loading, a three-layer feed-forward neural network is developed using the Lavenberg–Marquardt backpropagation-learning algorithm [14]. The MATLAB package is used for the development of present ANN models. The minimum number of hidden layers is considered, and in this case one hidden layer is sufficient to produce acceptable models. The neural network model has seven input nodes representing the concrete cylinder compressive strength f'_c, effective depth d, beam width b, shear span to depth ratio a/d, percentage longitudinal steel ratio p_t, percentage fiber volume fraction v_f and fiber aspect ratio l_f/d_f; one hidden layer with fourteen nodes and one output node representing the ultimate shear strength. The neural network model to be trained is presented in Fig. 6. Prior to exporting the data to the ANN for training, normalization of the data must be carried out which restricts the data range within an interval of 0–1. This is due to the use of the sigmoid nodal functions which restrict the output values between 0 and 1. Various normalization schemes have been adopted in the literature, however in the present training of network, normalization of a particular variable was performed using linear scaling of data as follows:

$$x_{i,norm} = \frac{x_{i,o}}{x_{\max}} \tag{14}$$

where $x_{i,o}$ and $x_{i,norm}$ are the ith components of the input vector before and after normalization respectively and x_{max} is the maximum value of all the components of the input vector before normalization. The scheme (Eq. (14)) is one of the simplest normalizing rules used in the present work and it allows the normalized data to modulate between the values of minimum/maximum ratio of an input parameter to 1.

Table 2
Range of data for network application.

Variable	Maximum	Minimum
f'_c (MPa)	62.0	20.0
b (mm)	225.5	100.0
d (mm)	300.0	100.0
a/d	1.240	0.40
p (%)	2.982	0.10
v_f (%)	3.350	0.50
l_f/d_f	113.0	48.0
V_u (kN)	1025.0	40.0
τ_u (MPa)	15.6	2.33

3.3. Implementation of neural network

As discussed earlier that construction of the network architecture is one of the most difficult tasks in the development of ANN models and it requires the selection of the input parameters and output parameters, which will restrict the number of the input and output nodes of the networks. For implementation of the present ANN model, the compressive strength of concrete is considered as one of the basic material properties of steel fiber reinforced concrete whereas the width and the effective depth of the corbel are related to the shearing area. In addition, the shear-span to depth ratio and the primary steel ratio affect the modes of failure. The volume fraction and the aspect ratio are the two important parameters of steel fibers in the concrete composite. Based on the previous analytical studies on shear strength of SFRC corbels the input variables considered in developing the ANN models are f'_c, b, d, a/d, p_t, v_f and l_f/d_f. Using a casual inference procedure, the relative importance of the input variables to the output can be ascertained. For the present networks, compressive strength of concrete is chosen as the most important parameter among all the input variables followed by width of the corbel section, effective depth of the corbel section, shear-span depth ratio, primary steel ratio, fiber volume fraction and finally aspect ratio of the fiber. Two

types of network architectures MA and MB considering different output parameters are considered in the study. Both the models MA and MB have the same input variables as mentioned above and one hidden layer with 14 neurons. Model MA is shear force (V_u) predictor and model MB is shear stress ($\tau_u = V_u/bd$) predictor. ANN simulations were conducted for the two different architectures, i.e., MA and MB using 730 numbers of training set data. During the training of the network models, the learning rates for the models were kept constant as 0.01. Lavenberg–Marquardt learning algorithm [14] was used to minimize the error function. The stopping criteria used for the training of networks were the different values of error goals, i.e., 0.02, 0.03, 0.04, 0.05, 0.06, 0.07 and 0.08. During the training, the convergence of network MA at different error goals was obtained without much difficulty while convergence at different error goals of network MB was achieved after many trials. As a trial if the number of nodes in hidden layer was reduced to less than 14 then in that case the network model MB did not achieve the target range of error goals. Therefore, the minimum number of hidden nodes was decided as 14 and was kept the same in the network model MA.

Different error goals ranging 0.02–0.08 were achieved during the successful learning of networks MA and MB. Now the networks are ready to be used to predict the results for a given set of input parameters. Though after training, the networks can try to yield the desired results as accurately as possible, it should be ensured that the networks can evaluate the desired function with unseen input data with minimum possible error. It is often possible that the established ANN model performs well on a training set data but the success is measured using the performance study carried out on the model with the unseen or independent data. This process of evaluating the functional performance of the trained networks with unseen data is called as testing of the neural networks. For testing the performance of the networks, a small tolerance limit should be allowed. In the present study, the training and the unseen or testing data are altogether different. While the input data sets are 730 in number obtained using the semi-characteristic equations, the testing set data are 55 in number collected from the experimental test results available in the literature [16–19,27]. For relative comparison of the performance of the network models MA and MB, the parameters like mean absolute error, root mean square error and Pearson coefficient of correlation were opted for better choice. During the testing stage, the predicted outputs by the different ANN models were compared at error goals 0.02–0.08 with respect to following error matrices; mean absolute error in percent (MAE), root mean square error in percent (RMSE) and Pearson coefficient of correlation (P), using 55 number of testing data sets, i.e., the experimental test results of SFRC corbels. The values of error matrices for ANN models MA and MB are presented in Table 3. The computation of error matrices are based on outputs of model MA in terms of shear force and those for model MB in terms of shear stress as compared with testing set data. While comparison of the outputs predicted by model MB with the experimental results (Table 4), shear stress τ_u of the test corbels is obtained as $\tau_u = V_u/bd$.

Table 3
Performance of network models at different error goal.

Designation of network model	Error goal	E_{avg} (%)	RMSE (%)	Pearson coefficient (P)
MA (Force predictor model)	0.02	13.332	18.890	0.831
	0.03	13.592	23.314	0.861
	0.04	10.449	14.252	0.946
	0.05	7.017	9.766	0.971
	0.06	7.133	9.696	0.950
	0.07	7.805	9.744	0.968
	0.08	9.437	12.677	0.939
MB (Stress predictor model)	0.02	9.726	14.876	0.940
	0.03	9.739	13.216	0.938
	0.04	11.147	14.772	0.891
	0.05	10.727	14.887	0.897
	0.06	7.831	10.479	0.962
	0.07	14.329	22.907	0.882
	0.08	13.194	18.194	0.921

Comparing the error matrices in Table 3 it is seen that the best result of MA models for shear force predictor is at error goal 0.05 whereas the best result of MB models of shear stress predictor is at error goal 0.06. The minimum values of error matrices at error goal = 0.05 for model MA are MAE = 7.017%, RMSE = 9.766% and P = 0.971 and those values at error goal = 0.06 for model MB are MAE = 7.831%, RMSE = 10.479% and P = 0.961. In both the networks MA and MB the minimum values of MAE achieved are less than 10% and the maximum values of P are greater than 0.95. The minimum values of RMSE for network model MA are less than 10% whereas for network model MB is slightly greater than 10%.

Based on the analysis of errors at different error goal of ANN models, the model MA at error goal 0.05 and model MB at error goal 0.06 had minimum values of MAE and RMSE and maximum values of P and thus selected for further validation. Henceforth in the text these models are simply written as MA and MB and they have to be tested on their performance with respect to other empirical or semi-empirical models for determining their ability to capture the inter-relationship of different parameters and simulate real physical process of shear behavior of SFRC corbels.

4. Study of the performance of the neural network model

4.1. Model predictions

The percentage error of the shear force predictor (model MA) and shear stress predictor (model MB) as compared with experimental results [16–19,27] or the testing set data are plotted in Fig. 7. It is observed from the figure that maximum and minimum errors in shear force prediction of corbels by model MA are about +15% and −40% whereas these errors are about +10% and −30% respectively in predicting shear stress of corbels by model MB. Excepting only one case that is corbel No. C6 (Table 4) the maximum negative percentage error is about 40% and 30% as predicted by ANN models MA and MB respectively. In general excepting very few cases the percentage error in predicting results by ANN model MA is +15% to −20% and by ANN model MB is +10% to −20% respectively. Moreover, the percentage error in predicting the shear strength by ANN model MB is more uniformly distributed showing superiority over the model MA.

4.2. Comparison with test results

Details of cross-sectional properties, experimental ultimate shear strength and ratio of experimental shear strength to computed values using analytical equations (7) or (8) [$F(\alpha)_{exp}/F(\alpha)_{cal}$], empirical equation [17] (V_{uexp}/V_{ucal}) and ANN models MA (V_{uexp}/V_{uANN}) and MB (τ_{uexp}/τ_{uANN}) have been presented in Table 4. Except corbel No. C6, it is observed that ratio of V_{uexp}/V_{uANN} (vide col. 14 of Table 4) and τ_{uexp}/τ_{uANN} (vide col. 15 of Table 4) are very close to 1.0 being average of 55 corbel tests are 0.960 and 0.949 respectively showing excellent performance by ANN models MA and MB. This shows the learning potential and predicting power of ANN models for complex behavior of SFRC corbels without shear reinforcement at shear failure.

Now the performance of network models MA and MB can be verified by simply varying one input parameter and all other input parameters are set to constant values. As such, results obtained from network models can be compared through Figs. 8–11 with experimental results, empirical equation given by Fattuhi [17] and semi-empirical equations (7) or (8). For the comparison of force

Table 4
Comparison with test results.

S. no.	Investigator	Corbel no.	a (mm)	b (mm)	d (mm)	A_s/bd (%)	f'_c (MPa)	Fiber properties		Vu_{expt} (kN)	$F(\alpha)_{exp}/F(\alpha)_{cal}$	V_{uexp}/V_{ucal}	V_{uexp}/V_{uANN}	τ_{uexp}/τ_{uANN}
								l_f/d_f	v_f (%)					
(1)	(2)	(3)	(4)	(5)	(6)	(7)	(8)	(9)	(10)	(11)	(12)	(13)	(14)	(15)
1	Hughes and	C_2	125	152	120.0	0.861	43.34	48	0.70	84.5	0.994	1.04	0.898	0.979
2	Fattuhi [27]	C_3	125	152	119	0.868	42.61	80	0.70	82.9	0.991	0.96	0.920	0.906
3		C_4	125	151	123	0.846	41.63	92	0.70	91.8	1.008	1.08	0.964	0.940
4		C_5	125	152	119	0.868	41.39	100	0.70	96.0	1.014	1.12	1.024	0.978
5		C_6	125	156	117	0.861	32.48	100	0.70	75.2	0.996	1.05	0.714	0.764
6	Fattuhi and	C_{27}	52.5	153	121	0.543	38.31	92	0.70	125.8	1.000	0.98	0.910	0.875
7	Hughes [18]	C_{28}	89	151	124	0.537	45.12	92	0.70	88.2	0.976	0.95	0.879	0.926
8		C_{29}	125	153	130	0.505	45.12	92	0.70	65.9	0.946	0.90	0.920	0.951
9		C_{30}	52.5	154	121.5	0.840	41.63	92	0.70	171.0	0.981	1.00	0.974	0.842
10		C_{31}	64.5	153	118	1.253	46.17	92	0.70	179.0	0.973	0.98	1.049	0.825
11		C_{32}	125	153	118	1.253	38.31	92	0.70	110.1	0.973	1.07	0.905	0.937
12	Fattuhi and	T_3	89	152	122	0.847	38.80	92	0.70	133.0	0.993	1.21	1.034	0.979
13	Hughes [19]	T_4	89	151	123	0.846	45.28	92	1.4	142.5	1.002	1.18	1.011	0.996
14		T_{10}	89	151	117	1.280	38.80	92	0.70	138.0	0.963	1.03	0.866	0.853
15		T_{11}	89	152	121	1.230	45.28	92	1.4	160.2	0.974	1.06	0.959	0.883
16		T_{12}	89	152	121	1.230	46.49	92	2.1	171.2	0.986	0.99	0.984	0.927
17	Fattuhi [16]	1	80	152.5	123	1.206	33.53	60	1.66	153.0	0.977	0.93	0.912	0.878
18		2	80	155	124	1.177	35.15	60	1.66	160.0	0.979	0.98	0.937	0.864
19		3	80	152.5	126	0.523	34.02	60	1.66	91.2	0.995	0.96	0.930	0.914
20		4	80	155	125	0.519	32.89	60	1.66	93.0	1.004	0.95	0.974	0.925
21		5	140	155	123	1.186	32.81	60	1.66	103.0	0.988	1.00	1.034	0.983
22		6	140	154.5	124	1.186	30.78	60	1.66	95.7	0.969	0.94	0.956	0.931
23		7	140	153	126	0.521	27.38	60	0.74	53.3	0.996	0.95	0.828	0.813
24		8	140	153	125.5	0.524	29.89	60	0.74	53.1	0.983	0.96	0.881	0.847
25		9	80	152.5	123	1.206	27.95	60	1.66	152.9	0.989	0.97	0.905	1.012
26		10	140	155.5	123	1.183	30.05	60	1.66	102.9	1.002	1.02	1.038	1.018
27		11	140	153	126	0.521	29.00	60	0.74	56.0	1.003	1.01	0.907	0.879
28		12	80	154	125	0.522	30.78	60	0.74	92.0	0.935	1.05	0.968	0.931
29		13	110	154.7	123	1.189	27.54	60	1.66	111.7	0.981	0.93	0.916	0.926
30		14	110	153.5	125	0.524	29.57	60	0.74	68.3	1.005	0.98	1.014	0.965
31		15	110	152.5	126	0.523	31.59	60	0.74	67.2	0.988	0.98	0.994	0.979
32		16	110	154.5	123.5	1.185	30.54	60	1.66	114.3	0.969	0.95	0.894	0.892
33		18	89	154	124.5	1.180	26.41	100	1.00	119.0	0.951	0.83	0.826	0.789
34	Fattuhi [17]	20	110	153	123.5	1.197	31.27	60	1.75	126.0	0.998	1.02	0.978	0.976
35		21	110	156	122	1.188	29.97	60	1.50	118.0	0.988	1.00	0.937	0.940
36		22	100	153	123	0.835	29.97	60	1.5	108.5	0.994	1.07	1.057	1.001
37		23	110	153	122.5	1.207	27.38	60	2.0	126.5	1.001	1.05	1.056	1.066
38		24	80	153	124	0.828	27.38	60	2.0	131.5	1.009	1.05	1.021	0.981
39		27	80	153.5	123.5	1.193	34.26	60	2.5	171.5	1.000	1.01	0.964	0.969
40		28	60	154	124	0.823	34.26	60	2.5	173.5	1.002	1.01	0.974	0.930
41		29	75	151.5	122.5	0.542	30.21	60	1.0	100.0	1.003	1.06	1.023	0.962
42		30	120	153.9	120.2	0.849	30.21	60	1.0	86.5	0.988	1.03	1.020	0.960
43		31	135	154.5	124	1.443	32.89	60	2.0	119.5	0.991	0.99	0.984	0.980
44		32	120	154	120.2	1.494	32.89	60	2.0	132.5	0.999	1.04	0.992	1.003
45		35	135	155.1	122.5	1.786	31.35	60	1.5	124.5	0.981	0.95	0.894	0.977
46		36	60	154.8	122	0.532	31.35	60	1.5	123.5	0.986	1.05	1.008	0.912
47		37	135	153.8	123.1	1.792	32.08	60	2.0	140.0	0.986	1.02	1.022	1.089
48		38	110	152.2	124	0.533	32.08	60	2.0	74.0	1.013	0.97	1.172	1.081
49		39	110	153.5	124	1.450	31.35	60	2.25	144.5	0.996	1.01	0.973	1.024
50		40	125	155.5	122.8	1.777	31.35	60	2.25	142.0	0.984	0.97	0.979	1.082
51		44	135	153.8	122.6	1.466	28.67	60	1.50	109.5	0.988	0.97	0.940	0.999
52		45	135	153.0	122.3	1.813	28.19	60	1.0	120.0	0.977	0.96	0.859	1.077
53		46	75	154.5	92	0.707	28.19	60	1.0	74.5	1.002	0.97	1.031	1.006
54		48	80	155.5	93.2	1.084	28.92	60	2.0	100.0	1.012	0.97	1.030	1.030
55		49	80	154.1	122.1	1.202	30.46	60	2.5	164.5	0.996	1.01	0.952	1.030
Avg.											0.989	1.003	0.960	0.949
S.D.											0.016	0.063	0.073	0.074

Notes: (i) The average compressive strength of 150 × 300 mm concrete cylinders is 81% of that for 100 mm cubes (described elsewhere [17]).
(ii) The values of $F(\alpha)_{cal}$ of col. (12) are computed either from Eq. (7) or (8) using convergence value of α which is evaluated from Eq. (1) and either Eq. (5) or (6).
(iii) V_{ucal} of col. 13 is computed using empirical equation given in [17].
(iv) The values of V_{uANN} and τ_{uANN} are taken from the outputs of network models MA and MB respectively.

predictor model MA, the shear stress is derived from the model output (V_u) as: $\tau_u = V_u/bd$ on the other hand, the shear stress predictor model MB directly yields values of shear strength at ultimate load.

Fig. 8 shows the effect of volume fraction on ultimate shear strength of corbel Nos. T10, T11 and T12 (Table 4). For these corbels shear span a = 89 mm, average value of p_t = 1.247% and average value of a/d ratio = 0.744. As observed experimentally, shear strength of corbel increases with the volume fraction of fibers. The same pattern is also exhibited by empirical equation [17], Eq. (7) or (8) and ANN models MA and MB. In this case however, model MB slightly overestimate the shear strength values and shows

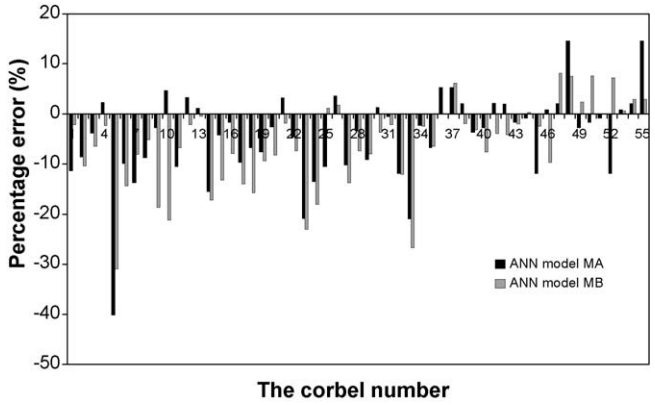

Fig. 7. Percentage error of network output.

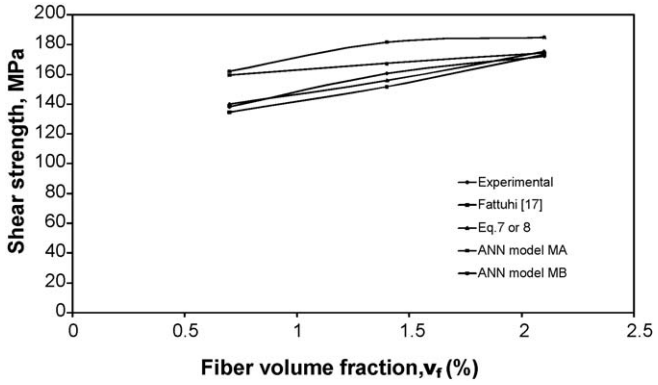

Fig. 8. Effect of volume fraction on ultimate shear strength of corbels No. T10, T11 and T12.

nonlinear relationship between shear strength and volume fraction that is similar to experimental results.

Effect of reinforcement index on shear strength of SFRC corbels is presented in Fig. 9 for corbel Nos. C2, C3, C4 and C5 (Table 4) where reinforcement index is equal to product of aspect ratio and volume fraction ($v_f \cdot l_f/d_f$) of steel fibers. In these corbels a = 125 mm, average value of a/d ratio = 1.04 and average value of p_t = 0.861%. From the figure it is observed that ANN model MB yields same pattern of results as obtained experimentally, using empirical equation [17] and Eq. (7) or (8) whereas shear force predictor model MA deviates after attaining the peak value of shear strength and it almost becomes constant after increasing the value of reinforcement index.

Fig. 10 shows the effect of primary reinforcement ratio p_t on ultimate shear strength of SFRC corbels for corbel Nos. 1, 3, 4 and 9

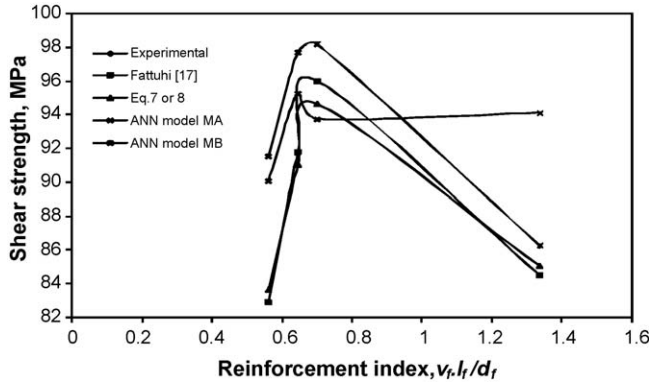

Fig. 9. Effect of reinforcement index on ultimate shear strength of corbels No. C2, C3, C4 and C5.

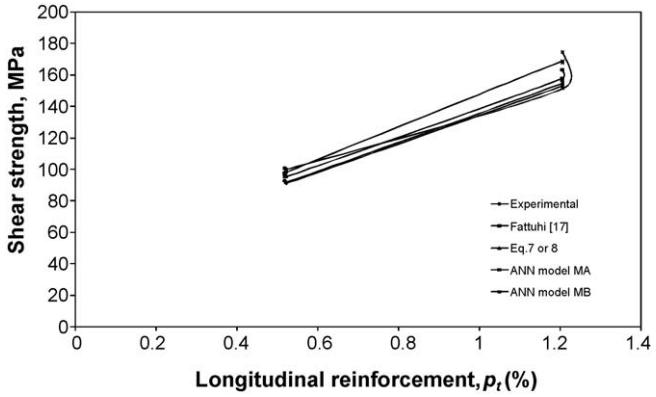

Fig. 10. Effect of longitudinal reinforcement ratio on ultimate shear strength of corbels No. 1, 3, 4 and 9.

(Table 4). For these corbels a = 80 mm, $v_f = 1.66\%$, l_f/d_f = 60, average value of a/d ratio = 0.644 and average of f'_c = 32.10 N/mm^2. Rate of increase in the shear strength of corbels using ANN models MA and MB, empirical equation given by Fattuhi [17] and Eq. (7) or (8) is almost same and consistent with the experimental results.

The most important parameter of corbels is a/d ratio that affects inversely the ultimate shear strength. For corbel Nos. C27, C28 and C29 (Table 4) the effect of a/d ratio on ultimate shear strength has been shown in Fig. 11. These corbels have $v_f = 0.77\%$, l_f/d_f = 92, average value of p_t = 0.528% and average of $f'_c = 42.85$ N/mm^2. From experimental results, it can be observed that the decrease in shear strength after increasing a/d ratio is nonlinear and the same variation can be seen from the results using ANN model MB, empirical equation by Fattuhi [17] and Eq. (7) or (8).

It is clear from the analysis that shear stress predictor model MB has better learnt than shear force predictor model MA the underlying mechanism and physical behavior of SFRC corbels subjected to vertical loading at shear failure. Therefore, the results obtained by ANN model MB which follows trends that are consistent with experimental results will be our qualitative evidence that the ANN model has learned to reproduce the physical process of shear failure of SFRC corbel without shear reinforcement. Shear strength predictions of the model MB are shown in Fig. 12 for both training and testing set data. From the figure, it is seen that training set data are being arranged in straight line of slope 45° and predicted shear strength as compared with experimental results are clustered around the line. This further shows evidence of excellent performance of ANN model MB.

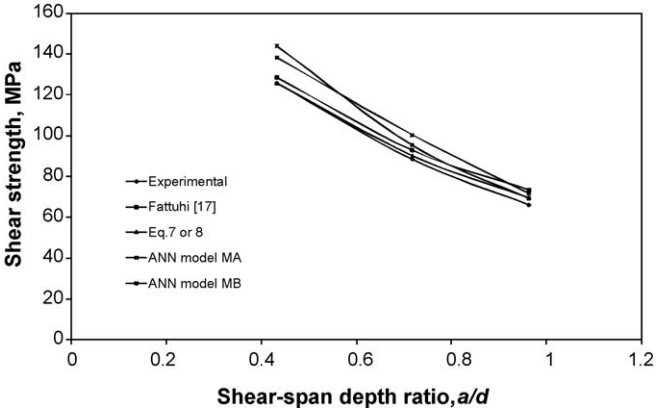

Fig. 11. Effect of shear span/depth ratio on ultimate shear strength of corbels No. 6, 7 and 8.

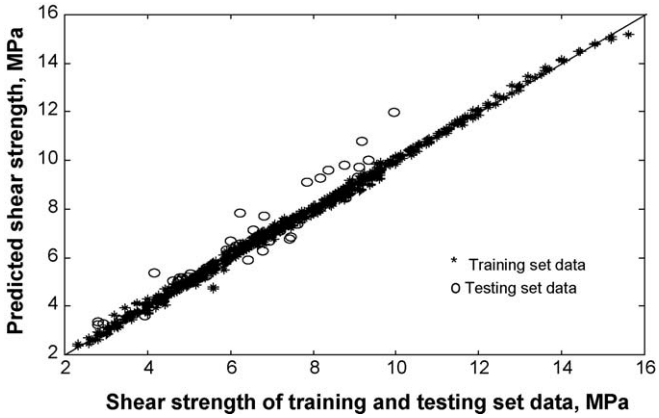

Fig. 12. Shear strength prediction of training and testing set data.

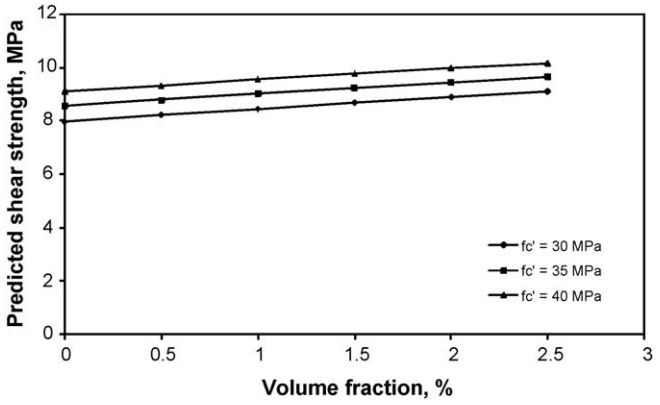

Fig. 14. Relationship between volume fraction and predicted shear strength at varying compressive strength of concrete.

4.3. Parametric study on shear strength

The physical behavior of SFRC corbels without shear reinforcement can be directly derived from the ANN model MB when one input parameter is altered and other input parameters are kept as constant. From the known fact the shear strength of SFRC corbel increases when compressive strength of concrete composite or longitudinal reinforcement or volume fraction of steel fibers either individually or jointly are increased whereas increase in shear span depth ratio causes decrease in shear strength. If the network has captured the physical process of shear behavior of SFRC corbels, its predictions should be sensitive to variation of each input parameter in consistent with the established facts. As such the following parametric studies have been carried out: relationship between volume fraction and predicted shear strength (Figs. 13 and 14), longitudinal steel ratio and predicted shear strength (Fig. 15) and shear-span depth ratio and predicted shear strength (Fig. 16) with varying compressive strength of concrete.

4.3.1. Influence of fiber volume fraction

Fig. 13 presents the behavior of predicted shear stress at failure for three values of compressive strength of concrete composite, i.e., $f'_c = 30$, 35 and 40 MPa. The other input parameters are b = 150 mm, d = 200 mm, a/d ratio = 0.8, p_t = 1.5% and l_f/d_f ratio = 90 and v_f being varied from 0.5 to 2.0%. From the figure, it is clear that rate of increase of shear strength at all three compressive strength of concrete is almost same and about 1.5% which is very marginal. This behavior of network model is also correct because in this case for a particular value of compressive strength of concrete, the value of compressive strength remains constant even though the value of volume fraction of fibers increases from 0.5 to 2.0%. As we know that compressive strength of fibred concrete is dependent on fiber volume fraction and it increases as volume fraction of fibers in concrete matrix increases. Therefore, the relationship of volume fraction on increasing values of compressive strength of fibrous concrete depending on volume fraction of fibers is shown in Fig. 14. In the figure the value of compressive strength of fibrous concrete (f_{cf}) is given by an empirical relation described elsewhere [45] as $f_{cf} = f'_c + 3.6\, v_f.\, l_f/d_f$, where f'_c = compressive strength of plain concrete matrix. In

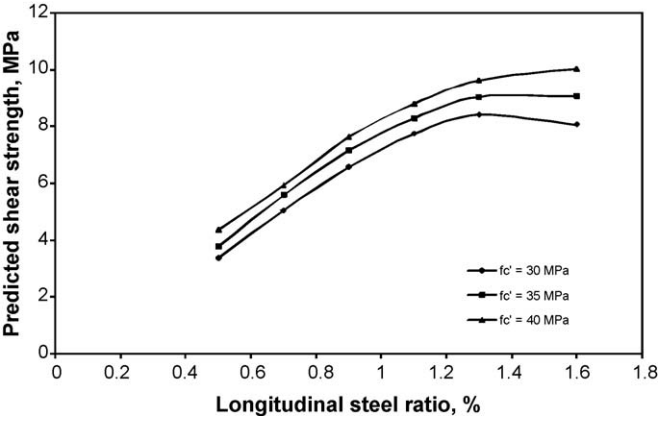

Fig. 15. Relationship between longitudinal steel ratio and predicted shear strength.

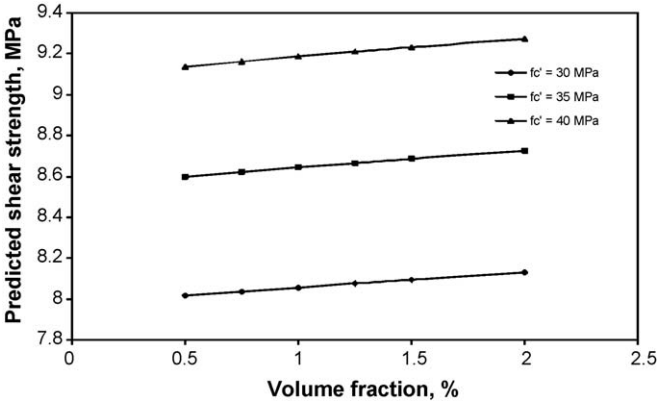

Fig. 13. Relationship between volume fraction and predicted shear strength at constant compressive strength of concrete.

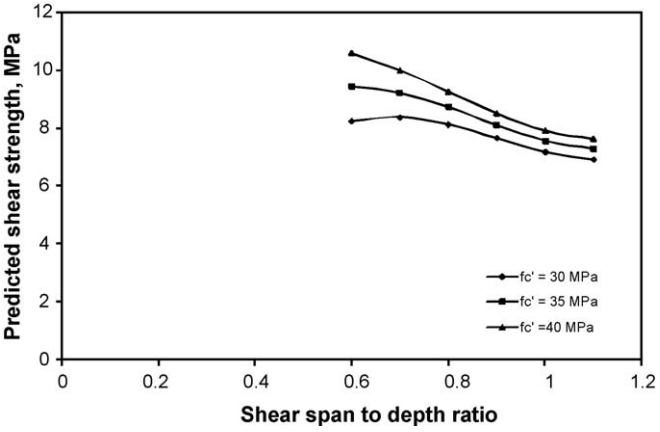

Fig. 16. Relationship between shear span-depth (a/d) ratio and predicted shear strength.

this case $f'_c = 30$, 35 and 40 MPa at $v_f = 0\%$ then f_{cf} = 38.1, 43.1 and 48.1 MPa at $v_f = 2.5\%$. Keeping all other input parameters the same as mentioned above the value of v_f is varied between 0 and 2.5% in Fig. 14. In the figure the rate of increase of shear strength is more at lower value of compressive strength of concrete for all three different types of concrete strength ($f'_c = 30$, 35 and 40 MPa at $v_f = 0\%$). The average increase in shear strength in this case is about 13% when v_f is increased up to 2.5%, which implies that shear strength finally depends on the increase of compressive strength of concrete when volume fraction of fibers in concrete is altered.

4.3.2. Influence of longitudinal reinforcement

Relationship between longitudinal steel ratio and predicted shear strength by ANN model MB at three different f'_c = 30, 35 and 40 MPa is shown in Fig. 15. The other input parameters are b = 150 mm, a/d = 0.7, $v_f = 2.0\%$, l_f/d_f = 90 and p_t being varied from 0.5 to 1.6% From figure it is seen that the value of p_t up to 1.3% there is sharp increase in shear strength of corbels and beyond that shear strength of corbel is almost constant for $f'_c = 30$ and 35 MPa whereas marginal increase is still found for $f'_c = 40$ MPa. For increase in the value of p_t from 0.5 to 1.3% the value of shear strength of corbel increases by 150.9% at $f'_c = 30$ MPa, 140.0% at $f'_c = 35$ MPa and 121.2% at $f'_c = 40$ MPa which shows the rate of increase of shear strength are more pronounced at lower values of compressive strength of concrete.

4.3.3. Influence of shear-span to depth ratio

Fig. 16 presents the relationship between the shear-span depth ratio and the predicted shear strength of SFRC corbels at three different values of compressive strength of concrete $f'_c = 30$, 35 and 40 MPa. Other input parameters for the study are b = 150 mm, d = 200 mm, p_t = 1.5%, $v_f = 2.0\%$, l_f/d_f = 90 and a/d ratio being varied from 0.6 to 1.1. From the figure, it is observed that there is decrease in shear strength of corbels at increasing value of a/d ratio. This decrease in shear strength is 15.81%, 22.77% and 28.06% at compressive strength of concrete f'_c = 30, 35 and 40 MPa respectively when a/d ratio increases from 0.6 to 1.1. The effect of a/d ratio is therefore more pronounced at higher values of compressive strength of concrete.

5. Summary and conclusions

In the present investigation, an attempt was made to study the learning and predicting capability of neural network models through simulating a complex and highly nonlinear problem in the field of structural engineering. Two ANN based models MA and MB were developed in the study for predicting the shear capacity of SFRC corbels without stirrups subjected to vertical loads and finally the model MB was adopted for the prospective parametric study because of its better predictive quality. The study of the influence of several parameters on the shear strength of SFRC corbels predicted by the ANN model MB was carried out in the previous section which showed an excellent performance of the network model. In the parametric study, the SFRC corbels made of three types of concrete compressive strength were considered to observe the variation in the predicted results according to the varied parameters. The results showed that the ANN could predict the shear strength of SFRC corbels in consistent with the expected experimental results. Though similar predictions can also be done using other empirical or semi-empirical equations available in the literature, the prediction of shear capacity of SFRC corbels using ANN approach can reveal some unknown and inherent behavior of the corbels at failure. One of the major advantages of the ANN model is that while formulating the problem, the network model does not require any simplifying assumptions unlike the developed semi-empirical characteristic equations (Appendix A). In addition, once the network model is established, no trial and error method is required during computation and hence the evaluation of shear strength of SFRC corbels can be done in relatively less time. While the developed empirical and semi-empirical equations available in the literature can be applied to the similar situation in which they have been derived, the ANN based model can be easily improved with the addition of new data enhancing the utility of the model in a broader way. The empirical or semi-empirical relations are generally developed based on the general inferences on the experimental results and the coefficient of the input parameters are evaluated according to a fixed rule whereas the ANN model learns from the data directly in a more natural way according to the given input and output data in an unknown functional manner. Therefore, shear strength prediction of SFRC corbels can be obtained in an exact nonlinear manner using the network model and hence ANN can be an effective and economic tool for performing the parametric study among the various parameters that affect real physical phenomenon in engineering analysis. This fact is evident from Figs. 13–16 in which the relationships between the shear strength of SFRC corbels and the different influencing parameters are constructed using ANN model MB. These relationships seem to be linear (Figs. 13 and 14) and nonlinear (Figs. 15 and 16) according to the natural predicting capacity of the network.

In the present work, it was seen that prediction of shear strength of steel fibrous reinforced concrete corbels without shear stirrups by neural network was excellent. Excepting stray in very few cases, the present model (MB) gave predictions of shear strength values within the error range of −20 to +10%. Although there is still a future scope to improve the ANN model, the present network model successfully simulates the effects of various parameters on shear strength of SFRC corbels without web reinforcement. From neural network application to SFRC corbels without web reinforcement the following conclusions may be drawn:

- The proposed ANN model very accurately predicted the experimental behavior for the ultimate shear capacity of test series of SFRC corbels subjected to vertical loading with various strength of concrete, primary steel ratios, shear span to depth ratios fiber volume fractions, fiber aspect ratios and geometrical sizes.
- Through parametric studies, it was confirmed that network model (MB) observed the shear stress at failure consistent with experimental results. A corbel with a higher compressive strength or and higher steel ratio or higher fiber volume fraction had higher shear capacity whereas higher shear span to depth ratio resulted in decrease in shear capacity of the SFRC corbels.
- Out of different input parameters, the effect of longitudinal reinforcement in the SFRC corbels seemed to be the most sensitive and even in slight increase of longitudinal reinforcement up to 1.3%, significant increase in the shear capacity of corbels was observed. The shear strength was almost constant beyond 1.3% value of longitudinal reinforcement. However, rate of increase of shear strength was more pronounced at lower values of compressive strength of concrete.

Appendix A. Derivation of shear strength characteristic curve for SFRC corbel

Assuming that at shear failure corbels reinforced with main bars and fibers exhibit multiple cracks on both sides of the columns as shown in Fig. 2. The first cracks located around, m, to appear are flexural cracks starting at junction of the tension face of the corbel and the face of the column. These cracks propagate about halfway, mn, through the depth of corbel at around half the ultimate shear

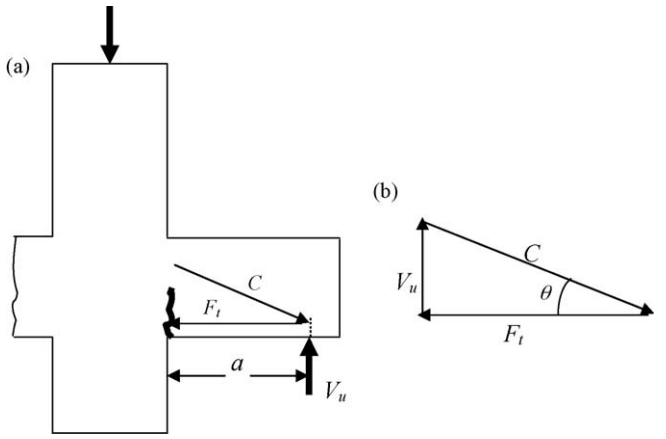

Fig. A1. (a) Development of strut-tie-action at shear failure. (b) Free body model of resultant forces.

load. After further loading multiple cracks appear around the inner edge of the load point, *p*, and progress towards the top re-entrant showing inclined cracks pattern, *pn*′. At ultimate capacity main bars of the corbel get yielded leading to failure about assumed mean neutral axis between points, *n* and *n*′ and critical section through, *mn*.

At shear failure, the strut-and-tie model (Fig. A1a) appears more suitable for simplified design. The free body diagram of resultant forces (Fig. A1b) shows the compressive strength of concrete in the compression strut and resultant tensile strength contributed by main bars and fiber-concrete composite as horizontal tie.

At the cracking load the stresses at the point *n*′ must satisfy a suitable fracture criterion, for instance, principal tension theory:

$$F_1\left(\frac{f_a}{f_c'}, \frac{v_a}{f_c'}\right) = \text{constant} \tag{A1}$$

where F_1 = is a functional notation. To compute the mean neutral axis depth *kd*, the following assumptions may be made as

1. The plane sections remain plane after bending.
2. There is no slip between concrete and steel.
3. The fiber composite contributes to the tensile strength of fibrous concrete.
4. Stress distribution in the compression bending zone follows the idealized stress strain curve for concrete as shown in Fig. A2.

Typical strain–stress curves for steel fiber reinforced concrete in compression for different types of steel wires are shown in ACI 544.4R [2]. In these curves, a substantial increase in the strain at peak stress can be noted. In flexural design of steel fibrous reinforced concrete beam based on ACI 544.4R [2] the maximum usable strain at extreme concrete compression fiber ε_{cc} is taken to be 0.003 and it is suggested that this strain may be conservative at flexural failure. Swamy and Al-Ta'an [46] recommended the ε_{cc} as 0.0035 in the analysis. From the test results [17,27] of fibrous concrete corbel with primary steel it is observed that concrete strain in compression at maximum load is not a constant value and it varies between 0.001185 and 0.0059 for different test corbels depending upon their test conditions and cross-sectional properties. Based on these observations, a plasticity coefficient α was introduced [32] after suitable modification of the work [40]. The value of α may mainly depend on the cross-sectional properties of the test corbel and *a*/*d* ratio. It would be therefore, reasonable to assume that steel fibrous concrete appears to be plastic at a strain value of 0.002 and the strain at extreme concrete compression fiber at maximum load depends on final value of plasticity coefficient.

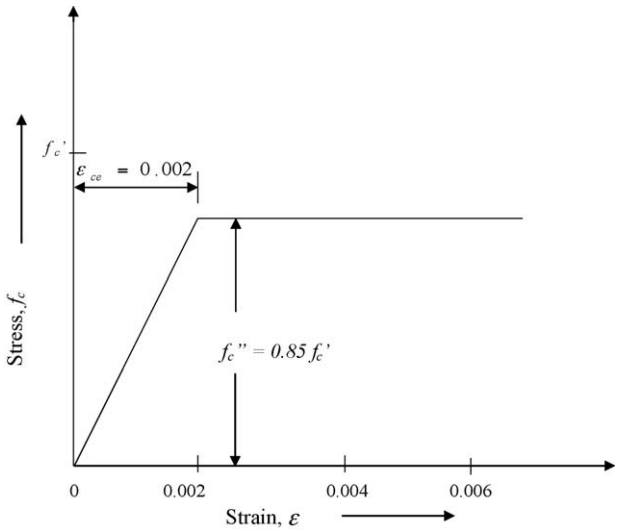

Fig. A2. Idealized stress–strain curve for concrete.

The idealized strain and stress distribution across the corbel depth at shear failure is shown in Fig. A3. The figure is self-explanatory. Neglecting tensile force contributed by fiber concrete below effective cover, at shear failure the following equation can be written from horizontal equilibrium (Fig. A3).

Total compressive force = Total tensile force

$$C = F_{st} + F_{ft} \tag{A2}$$

$$k_1 k f_c'' bd\cos\theta = A_s f_s + \sigma_{cu}(d - kd)b \tag{A3}$$

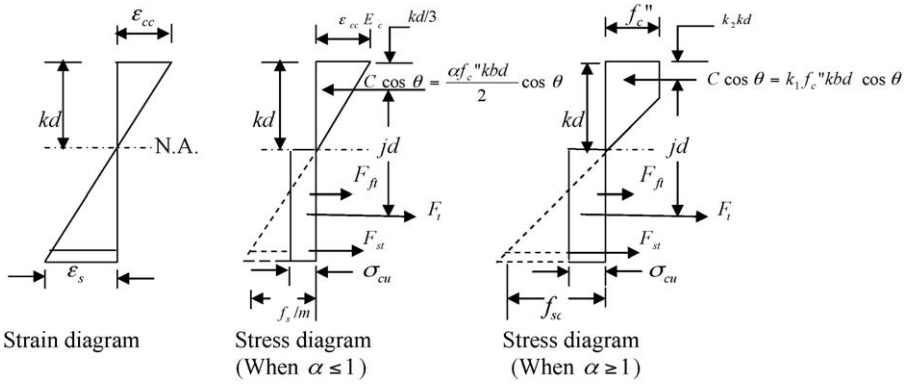

Fig. A3. Idealized strain and stress distribution at shear failure.

Defining α = plasticity coefficient $\varepsilon_c/\varepsilon_{ce}$, where ε_{cc} = top concrete strain at cracking load at critical section and ε_{ce} = strain at which concrete is assumed to become plastic = 0.002 (from Fig. A2). From vertical equilibrium of forces (Fig. A1b), the following equation can be written as

$$C\sin\theta = V_u \tag{A4}$$

Further, the following equation can expressed from moment of external and internal forces about tensile force at critical section

$$C\cos\theta\, jd = V_u a \tag{A5}$$

where $j = 1 - k_2 k$; $f_c'' = 0.85\ f_c'$ and the tensile strength of fiber concrete [46] can be expressed as

$$\sigma_{cu} = \eta_o \eta_b \eta_l 2\tau \left(\frac{l_f}{d_f}\right) v_f \tag{A6}$$

In which, η_o = fiber orientation factor = 0.41, η_b = bond efficiency factor [21] = $l_f/2k_b d_f\{1.5 - l_f/2k_b d_f(1 - l_f/8k_b d_f)\}$ and k = bond length coefficient [21] = grip length/d_f = 58.

The value of length correction factor η_l given by Cox [12] renders a conservative assumption and therefore, in general a suitable value of the range 1/3 to 1/6 of η_l responds well with the test data. In this analysis, consider $\eta_l = 1/3$ and $\tau = 2.44\ \mathrm{N/mm^2}$ [46]; Eq. (A3) can be rearranged to form Eq. (1). In which, $\cos\theta = 1/[1 + \{(1 - k_2 k)d/a\}^2]^{1/2}$ and $E_c = 0.85\, f_c'/0.002$ (from Fig. A2). The value of k_1 and k_2 may be obtained in the form of Eq. (2) and (3) from idealized stress–strain curve for fibrous concrete (Fig. A3).

As too much refinement in the analysis is unnecessary, in view of the complexities involved in the problem shear stress distribution on the critical section is dependant on the cross-section, the nature of longitudinal stress-distribution along the depth which may conveniently be represented by α and coefficient γ. This signifies the stretch of the crack at shear cracking, being a time dependant parameter and depends on the composition and homogeneity of concrete, the size of aggregate particles, etc. Neglecting the shear resistance capacity of tensile steel and interlocking action of aggregate particles, the average shear stress near the critical stress field is expressed as

$$v_a = F_2\left[\frac{V_u}{kbd}, \alpha, f_c', \gamma, \sigma_{cu}\right] \tag{A7}$$

in which, F_2 is a functional notation and V_u = shear force at shear cracking at the critical section. Similarly,

$$f_a = F_3\left[\frac{V_u a}{kbd^2\cos\theta}, \alpha, f_c', \gamma, \sigma_{cu}\right] \tag{A8}$$

where F_3 is a functional notation. Assuming highly indeterminate coefficient γ to be constant and j is a function of k and α, Eq. (A2) in conjunction with Eqs. (A7) and (A8) yields that:

$$F_4\left[\frac{V_u a}{kbd^2\cos\theta}, \alpha, f_c', \sigma_{cu}\right] = \text{constant} \tag{A9}$$

For a particular corbel test, the unknown quantities are k and α. Further Eqs. (4)–(6) can be obtained using Eq. (A4).

For a particular corbel test, values of k and corresponding α at observed V_u may be calculated from Eqs. (1)–(3), (5) and (6), by trial and error, assuming a suitable value of α. In the present calculation nonlinear Eq. (10) is solved for the value of k for each given value of α with the help of computer program by Newton–Raphson method of numerical analysis. On careful examination of the computed values of the parameters, such as V_u/kbd, a/d, $\cos\theta$, f_c' and α for each test specimens, Eq. (A9) was found to be most agreeable to the test data in the following form:

$$\frac{V_u}{kbd} \times \frac{a}{d} \times \frac{1}{f_c''} \times \frac{1}{\cos\theta} = F_5(\alpha) \tag{A10}$$

in which $F_5(\alpha)$ is a functional notation. Eqs. (7) and (8) are obtained when the non-dimensional quantities $V_u a/kbd^2\, f_c''\cos\theta$ are plotted against α for all test corbels [16–19,27] as shown in Fig. 3. The value of $F(\alpha)$ vide column 12 of Table 4 shows that Eqs. (7) and (8) called as corbel characteristic equations are in excellent agreement with the test results. Finally, shear strength characteristic Eqs. (9) and (10) are obtained using Eqs. (4), (7) and (8).

References

[1] H.M.S. Abdul-Wahab, Strength of reinforced concrete corbels with fibers, ACI Structural Journal 86 (1) (1989) 60–66.
[2] ACI Committee 544, Design considerations for steel fiber reinforced concrete (ACI 544.4R-88), ACI Structural Journal 85(5) (1988) 563–580.
[3] ACI Committee 318, Building code requirements for reinforced concrete (ACI 318-95), American Concrete Institute, Detroit, MI 48219, 1995.
[4] J.A. Abdallaa, A. Elsanosib, A. Abdelwahab, Modeling and simulation of shear resistance of R/C beams using artificial neural network, Journal of the Franklin Institute 344 (2007) 741–756.
[5] B.B. Adhikary, H. Mutsuyoshi, Artificial neural networks for the prediction of shear capacity of steel plate strengthened RC beams, Construction and Building Materials 18 (2004) 409–417.
[6] C. Bilim, C.D. Atis, H. Tanyildizi, O. Karahan, Predicting the compressive strength of ground granulated blast furnace slag concrete using artificial neural network, Advances in Engineering Software 40 (2009) 334–340.
[7] H. El-Chabib, M. Nehdi, A. Said, Predicting shear capacity of NSC and HSC slender beams without stirrups using artificial intelligence, Computers and Concrete 2 (1) (2005) 79–96.
[8] P.H. Chuang, A.T.C. Goh, X. Wu, Modeling the capacity of pin-ended slender reinforced concrete columns using neural network, Journal of Structural Engineering ASCE 124 (7) (1998) 830–838.
[9] A. Cladera, A.R. Mari, Shear design procedure for reinforced normal and high-strength concrete beams using artificial neural networks. Part I. Beams without stirrups, Engineering Structures 26 (2004) 917–926.
[10] A. Cladera, A.R. Mari, Shear design procedure for reinforced normal and high-strength concrete beams using artificial neural networks. Part II. Beams with stirrups, Engineering Structures 26 (2004) 927–936.
[11] A. Cladera, A.R. Mari, Experimental study on high-strength concrete beams failing in shear, Engineering Structures 27 (2005) 1519–1527.
[12] H.L. Cox, The elasticity and strength of paper and other fibrous materials, British Journal of Applied Physics 3 (1952) 72–79.
[13] F. Demir, Prediction of elastic modulus of normal and high strength concrete by artificial neural networks, Construction and Building Materials 22 (2008) 1428–1435.
[14] H. Demuth, M. Beale, Neural Network Toolbox User's Guide, The Mathworks Inc., 1998.
[15] N.I. Fattuhi, Corbels with shear reinforcement in the form of stirrups or fibres, in: Proceedings third RILEM International Symposium on Development of Fibre Reinforced Cement and Concrete, vol. 2, University of Sheffield, July, 1986, paper No. 8.8.
[16] N.I. Fattuhi, Column-load effect on reinforced concrete corbels, Journal of Structural Engineering ASCE 116 (1) (1990) 188–197.
[17] N.I. Fattuhi, Strength of SFRC corbels subjected to vertical load, Journal of Structural Engineering ASCE 116 (3) (1990) 701–718.
[18] N.I. Fattuhi, B.P. Hughes, Reinforced steel fiber concrete corbel with various shear span-to-depth ratios, ACI Materials Journal 86 (6) (1989) 590–596.
[19] N.I. Fattuhi, B.P. Hughes, Ductility of reinforced concrete corbels containing either steel fibers or stirrups, ACI Structural Journal 86 (6) (1989) 644–651.
[20] I. Flood, L. Muszynski, S. Nandy, Rapid analysis of externally reinforced concrete beams using neural networks, Computers and Structures 79 (2001) 1553–1559.
[21] S. Ghosh, C. Bhattacharya, S.P. Ray, Effective wire spacing in steel fibre reinforced concrete, Journal the Institution of Engineers (India) CI 69 (1989) 222–227.
[22] A.T.C. Goh, Prediction of ultimate shear strength of deep beams using neural networks, ACI Structural Journal 92 (1) (1995) 28–32.
[23] N.H. Guang, W.J. Zong, Prediction of compressive strength of concrete by neural networks, Cement and Concrete Research 30 (2000) 1245–1250.
[24] M.N.S. Hadi, Neural networks applications in concrete structures, Computers and Structures 81 (2003) 373–381.
[25] T. Hagberg, Design of concrete brackets: on the application of the truss analogy, ACI Journal 80 (1) (1983) 3–12.
[26] S. Haykin, Neural Network: A Comprehensive Foundation, 2nd ed., Prentice-Hall of India Private Limited, New Delhi, India, 2004.
[27] B.P. Hughes, N.I. Fattuhi, Reinforced steel and polypropylene fiber concrete corbel tests, The Structural Engineer London 67 (4) (1989) 68–72.
[28] W. Ji-Zong, H.G. Ni, H. Jin-Yun, The application of automatic acquisition of knowledge to mix design of concrete, Cement and Concrete Research 29 (1999) 1875–1880.

[29] S. Jung, K.S. Kim, Knowledge-based prediction of shear strength of concrete beams without shear reinforcement, Engineering Structures 30 (2008) 1515–1525.
[30] J. Kasperkiewicz, J. Racz, A. Dubrawski, HPC strength prediction using artificial neural network, Journal of Computing in Civil Engineering ASCE 9 (4) (1995) 279–284.
[31] J.I. Kim, D.K. Kim, M.Q. Feng, F. Yazdani, Application of neural networks for estimation of concrete strength, Journal of Materials in Civil Engineering ASCE 16 (3) (2004) 257–264.
[32] S. Kumar, Shear strength of reinforced fibrous concrete corbels without shear reinforcement, Journal the Institution of Engineers (India) 85 (2004) 202–212.
[33] S.-C. Lee, Prediction of concrete strength using artificial neural networks, Engineering Structures 25 (2003) 849–857.
[34] S.C. Lee, S.K. Park, B.H. Lee, Development of the approximate model for the stub-girder system using neural network, Computers and Structures 79 (2001) 1013–1025.
[35] M.Y. Mansour, M. Dicleli, J.Y. Lee, J. Zhang, Predicting the shear strength of reinforced concrete beams using artificial neural networks, Engineering Structures 26 (2004) 781–799.
[36] A. Mukherjee, J.M. Deshpande, Application of artificial neural networks in structural design expert systems, Computers and Structures 54 (3) (1995) 367–375.
[37] A.W.C. Oreta, K. Kawashima, Neural network modeling of confined compressive strength and strain of circular concrete columns, Journal of Structural Engineering ASCE 129 (4) (2003) 554–581.
[38] A.W.C. Oreta, Simulating Size effect on shear strength of RC beams without stirrups using neural network, Engineering Structures 26 (2004) 681–691.
[39] P. Park, T. Paulay, Reinforced Concrete Structures, A Wiley-Interscience Publication, John Wiley & Sons, New York, 1975.
[40] K. Paswan, S. Kumar, S.P. Ray, Shear strength of reinforced fibrous concrete beams without web reinforcement, Journal of the Bridge and Structural Engineer, Indian National group of IABSE, New Delhi 30 (3) (2000) 17–29.
[41] B.K. Raghu Prasad, H. Eskandari, B.V.V. Reddy, Prediction of compressive strength of SCC and HPC with high volume fly ash using ANN, Construction and Building Materials 23 (2009) 117–128.
[42] S. Rajasekaran, R. Amalraj, Predictions of design parameters in civil engineering problems using SLNN with a single hidden RBF neuron, Computers and Structures 80 (2002) 2495–2505.
[43] A. Sanad, M.P. Saka, Prediction of ultimate shear strength of reinforced concrete deep beams using neural networks, Journal of Structural Engineering ASCE 127 (7) (2001) 818–828.
[44] M. Sarıdemir, Prediction of compressive strength of concretes containing metakaolin and silica fume by artificial neural networks, Advances in Engineering Software 40 (2009) 350–355.
[45] P. Soroushian, C.D. Lee, Constitutive modeling of steel fibre reinforced concrete under direct tension and compression, in: Proceedings of the International Conference on Recent Development in Fibre Reinforced Cement and Concrete, Cardiff, (1989), pp. 363–377.
[46] R.N. Swamy, S.A. Al-Ta'an, Deformation and ultimate strength in flexure of reinforced concrete beams made with steel fibres concrete, ACI Journal Title 78 (36) (1981) 395–405.
[47] G. Trtnik, F. Kavčič, G. Turk, Prediction of concrete strength using ultrasonic pulse velocity and artificial neural networks, Ultrasonics 49 (2009) 53–60.
[48] I.B. Topçu, M. Sarıdemir, Prediction of properties of waste AAC aggregate concrete using artificial neural network, Computational Materials Science 41 (2007) 117–125.
[49] Z. Waszczyszyn, L. Ziemiański, Neural networks in mechanics of structures and materials-new results and prospects of applications, Computers and Structures 79 (2001) 2261–2276.
[50] I.-C. Yeh, Modeling concrete strength with augment-neuron networks, Journal of Materials in Civil Engineering ASCE 10 (4) (1998) 263–268.